International Journal of Greenhouse Gas Control 18 (2013) 224–236

Contents lists available at ScienceDirect

International Journal of Greenhouse Gas Control

journal homepage: www.elsevier.com/locate/ijggc

CO_2 soil flux baseline at the technological development plant for CO_2 injection at Hontomin (Burgos, Spain)

J. Elío[a,b,*], B. Nisi[c], M.F. Ortega[b], L.F. Mazadiego[b], O. Vaselli[d,e], F. Grandia[f]

[a] Fundación Ciudad de la Energía (CIUDEN), Ponferrada, León, Spain
[b] ETS Ingenieros de Minas Universidad Politécnica de Madrid (UPM), Madrid, Spain
[c] CNR-IGG Institute of Geosciences and Earth Resources, Pisa, Italy
[d] Department of Earth Sciences, Florence, Italy
[e] CNR-IGG Institute of Geosciences and Earth Resources, Florence, Italy
[f] AMPHOS21, Barcelona, Spain

ARTICLE INFO

Article history:
Received 27 April 2013
Received in revised form 5 July 2013
Accepted 23 July 2013

Keywords:
CO_2 storage
Geochemical baseline
CO_2 soil fluxes
Hontomín

ABSTRACT

From the end of 2013 and during the following two years, 20 kt of CO_{2sc} are planned to be injected in a saline reservoir (1500 m depth) at the Hontomín site (NE Spain). The target aquifers are Lower Jurassic limestone formations which are sealed by Lower Cretaceous clay units at the Hontomín site (NE Spain). The injection of CO_2 is part of the activities committed in the Technology Development phase of the EC-funded OXYCFB300 project (European Energy Program for Recovery – EEPR, http://www.compostillaproject.eu), which include CO_2 injection strategies, risk assessment, and testing and validating monitoring methodologies and techniques.

Among the monitoring works, the project is intended to prove that present-day technology is able to monitor the evolution of injected CO_2 in the reservoir and to detect potential leakage. One of the techniques is the measurement of CO_2 flux at the soil–atmosphere interface, which includes campaigns before, during and after the injection operations.

In this work soil CO_2 flux measurements in the vicinity of oil borehole, drilled in the eighties and named H-1 to H-4, and injection and monitoring wells were performed using an accumulation chamber equipped with an IR sensor. Seven surveys were carried out from November 2009 to summer 2011. More than 4000 measurements were used to determine the baseline flux of CO_2 and its seasonal variations.

The measured values were low (from 5 to 13 g m^{-2} day^{-1}) and few outliers were identified, mainly located close to the H-2 oil well. Nevertheless, these values cannot be associated to a deep source of CO_2, being more likely related to biological processes, i.e. soil respiration. No anomalies were recognized close to the deep fault system (Ubierna Fault) detected by geophysical investigations. There, the CO_2 flux is indeed as low as other measurement stations. CO_2 fluxes appear to be controlled by the biological activity since the lowest values were recorded during autumn-winter seasons and they tend to increase in warm periods. Two reference CO_2 flux values (UCL_{50} of 5 g m^{-2} d^{-1} for non-ploughed areas in autumn–winter seasons and 3.5 and 12 g m^{-2} d^{-1} for in ploughed and non-ploughed areas, respectively, in spring–summer time, and UCL_{99} of 26 g m^{-2} d^{-1} for autumn–winter in not-ploughed areas and 34 and 42 g m^{-2} d^{-1} for spring–summer in ploughed and not-ploughed areas, respectively) were calculated. Fluxes higher than these reference values could be indicative of possible leakage during the operational and post-closure stages of the storage project.

1. Introduction

The European Energy Program for Recovery (EEPR) selected in 2009 the OXYCFB300 Compostilla Project (Lupion et al., 2011) as one of the six CCS Demo projects which include a Technology Development phase, where pilot facilities for CO_2 capture, transport and storage will be built and operated, giving a valuable input to the demo phase (European Energy Program for Recovery–EEPR, http://www.compostillaproject.eu). One of the main goals are the development and optimization of feasible injection strategies, establishment of monitoring methodologies to verify the evolution of the injected CO_2 and assure its safety, investigation and understanding of the long term processes that control CO_2 geological storage, to demonstrate the viability of the sequestration and storage of CO_2 to reduce the emissions of this

* Corresponding author at: Fundación Ciudad de la Energía (CIUDEN), Ponferrada, León, Spain. Tel.: +34 987 457 454; fax: +34 987 419 570.
E-mail addresses: javielio@qyc.upm.es, javier.elio@ciuden.es (J. Elío).

1750-5836/$ – see front matter © 2013 Elsevier Ltd. All rights reserved.
http://dx.doi.org/10.1016/j.ijggc.2013.07.013

greenhouse gas to the atmosphere and mitigate its potential climate changes.

The storage area of the project is located close to the village of Hontomín (Burgos, northern Spain) where approximately 20,000 tons of CO_2 are planned to be injected into a saline aquifer at 1500 m depth (Ogaya et al., 2013) from the end of 2013 and during the following two years. This Technology Development Plant on CO_2 Storage (TDP) is owned and operated by the Fundación Ciudad de la Energía (CIUDEN), which belongs to the Spanish Government.

To ensure that the containment of CO_2 in the saline aquifer is effective, monitoring campaigns are carried out to detect potential leakage and, if occurring, to identify and quantify it. Monitoring programs are performed during the injection stage and after the closure of the storage. For a correct interpretation and quantification of the leakage, it is a priority to establish a pre-injection, undisturbed-state characterization (called *baseline*) of the area affected by CO_2 storage, not only at the reservoir level but also at shallow depth, surface and atmosphere. Baseline studies thus include a large number of geophysical and geochemical methodologies (e.g. Arts and Winthaeoen, 2005; Klusman, 2011).

In 1993 the International Geological Correlation Program (IGCP Project 360) officially introduced the term "geochemical baseline". It refers to the natural variation in concentration of a certain element or compound in the superficial environment (e.g. Salminen and Tarvainen, 1997; Salminen and Gregorauskien, 2000). The term specifies the content and statistical range of an element/compound in the superficial environment at a given point in time (Salminen and Gregorauskien, 2000; Frattini et al., 2006; Albanese et al., 2007). It includes the geogenic natural concentrations (natural background) and the diffuse anthropogenic contribution in different matrices, e.g. soils (Tarvainen and Kallio, 2002; Cicchella et al., 2005; Frattini et al., 2006; Albanese et al., 2007).

This definition is particularly relevant when monitoring of onshore carbon capture and storage (CCS) areas is performed. The detection of CO_2 leakages is challenging since it is generally unpredictable since it may occur shortly after the injection or be delayed from few to thousands years. As a consequence, near-surface CO_2 gas geochemistry, i.e. gas flux at the soil–atmosphere interface, can be regarded as an important tool to distinguish anomalies related to CO_2 leakage from near-surface biological reactions, e.g. Beaubien et al. (2013). Nevertheless, an appropriate definition of the CO_2 geochemical baseline based on a correct statistical approach is required.

The determination of the composition and the flux of soil gases are quite well established techniques, which are regularly used in the baseline studies for characterizing of a CO_2 injection site (IEA-GHG 2004; IPCC, 2006; NETL, 2009; USEPA, 2010). In this work, CO_2 soil fluxes in the site of Hontomín were measured by the accumulation chamber technique, widely used in geological storage of CO_2 projects (e.g. Klusman, 2003a; 2003b; 2005; 2011; Förster et al., 2006; Leuning et al., 2008; Beaubien et al., 2013).

The main aims of this study are those to: (i) assess the seasonal variability of CO_2 soil flux; (ii) evaluate the CO_2 output and (iii) define a CO_2 geochemical baseline to be used as background for future monitoring studies, to be undertaken during the injection and post-injection phases.

2. Geology and structure of the Hontomín area

The TDP of Hontomín area belongs to the Basque-Cantabrian Domain (Fig. 1), flanked by the Ebro and Duero basins, and is characterized by Triassic to Quaternary sedimentary rocks (IGME, 1991). Hontomín is bordered to the SW by the NW-SE-oriented Ubierna Fault, to the north by the Poza de la Sal salt dome, and to the east by the Ebro Basin (e.g. Tavani et al., 2011; Quintà et al., 2012). The target aquifer for CO_2 injection consists of limestones and dolostones of Jurassic age located at 1450 m depth. The reservoir formation shows secondary porosity (>12%) filled by saline fluids (up to 30 g/L as NaCl, Buil et al., 2012; Nisi et al., 2013). According to Alcalde et al. (2013), the minimum thickness of the reservoir Unit is 100 m. The seal formation is made up of clays and marls whose thickness is between 314 and 545 m. 2D seismic reflection images and borehole logs indicate that the reservoir has a dome-like structure, roughly 5 km × 3 km (Alcalde et al., 2013). The core of the Hontomín dome consists of the Keuper Facies, overlain by evaporites, dolomites and marls (Puerto de la Palombera Formation; Pujalte et al., 2004; Quesada et al., 2005). Jurassic shallow marine carbonates and hemipelagic carbonate and marls and Upper Jurassic to Lower Cretaceous clays, sandstone and carbonate rocks, unconformably set on the marine rocks, underlain siliciclastic rocks that refer to the Weald, Escucha, and Utrillas Facies. The outcropping rocks in the Hontomín area are mainly Upper Cretaceous carbonates and Cenozoic detritic and lacustrine rocks. The understanding of the underground geology was supported by log data from oil exploration wells drilled in the 1980s, numbered H-1, H-2, H-3 and H-4 (Quesada et al., 1993, 1995, 1997; Quesada and Robles, 1995; Permanyer et al., 2013).

The Hontomín site is located in a closed anticlinal dome delimited by two normal faults of a roughly E-W oriented trend. The fault situated in the northern flank of the anticlinal has a WNW-ESE trend and dips to the north. This fault, crossed by the H-1 drill, is named Fault HNT1. In the southern flank, a WNW-ESE oriented normal fault (Fault HNT3) dipping to the south was crossed by the test drill H-3 (Tavani et al., 2011). Geophysical data suggest that the northernmost fault is buried and does not likely represent a CO_2 leakage pathway, whereas the southernmost fault may reach the surface (Alcalde et al., 2013).

The injection pilot plant at Hontomín will consist of two wells (H-I, H-A) with an approximate depth of 1600 m each (Fig. 1). The H-I will be used as injection well, while the H-A well will be a monitoring well to investigate the evolution of the CO_2 plume. These wells are expected to be equipped with pressure-temperature (P/T) and pore pressure sensors, fluid sampling from the injection level and detectors for the acquisition of seismic, magnetotelluric, geochemical and geoelectrical data.

3. Materials and methods

Carbon dioxide soil fluxes were measured using the accumulation chamber method (e.g. Chiodini et al., 1998; Cardellini et al., 2003; Klusman, 2011), which is based on the measurement of the CO_2 concentrations with time by an inverted chamber placed on the ground. The accumulation chamber device consists of: (i) a metal cylindrical chamber with an inlet net area and inner volume of 3.14×10^{-2} m^2 and 3.06×10^{-3} m^3, respectively, (ii) an Infra-Red (IR) spectrophotometer (Licor® Li-820, infra-red sensor detector, measuring range of 0–20,000 ppm, accuracy of 4% of reading), (iii) an analog-digital (AD) converter, and (iv) a palmtop computer (PC).

A low-flux pump (20 mL s^{-1}) continuously convoys the soil gas from the chamber to the IR. To minimize the disturbance effects due to changes of barometric conditions, the soil gas is re-injected into the chamber. The soil CO_2 flux is calculated on the basis of the measured CO_2 concentration increment inside the chamber in time (dC_{CO_2}/dt). To express the flux in g m^{-2} d^{-1} the following conversion is applied:

$$\Phi(\text{g m}^{-2}\,\text{day}^{-1}) = \frac{dC}{dt} \cdot \frac{V}{A} \cdot \frac{86,400}{1000} \cdot \frac{P \cdot PM}{R \cdot T}$$

where dC/dt [ppm s^{-1}] refers to the concentration curve over time, V [m^3] is the net volume of the chamber (including the volume of the sensor, pump and connection tubes), A [m^2] is the area of

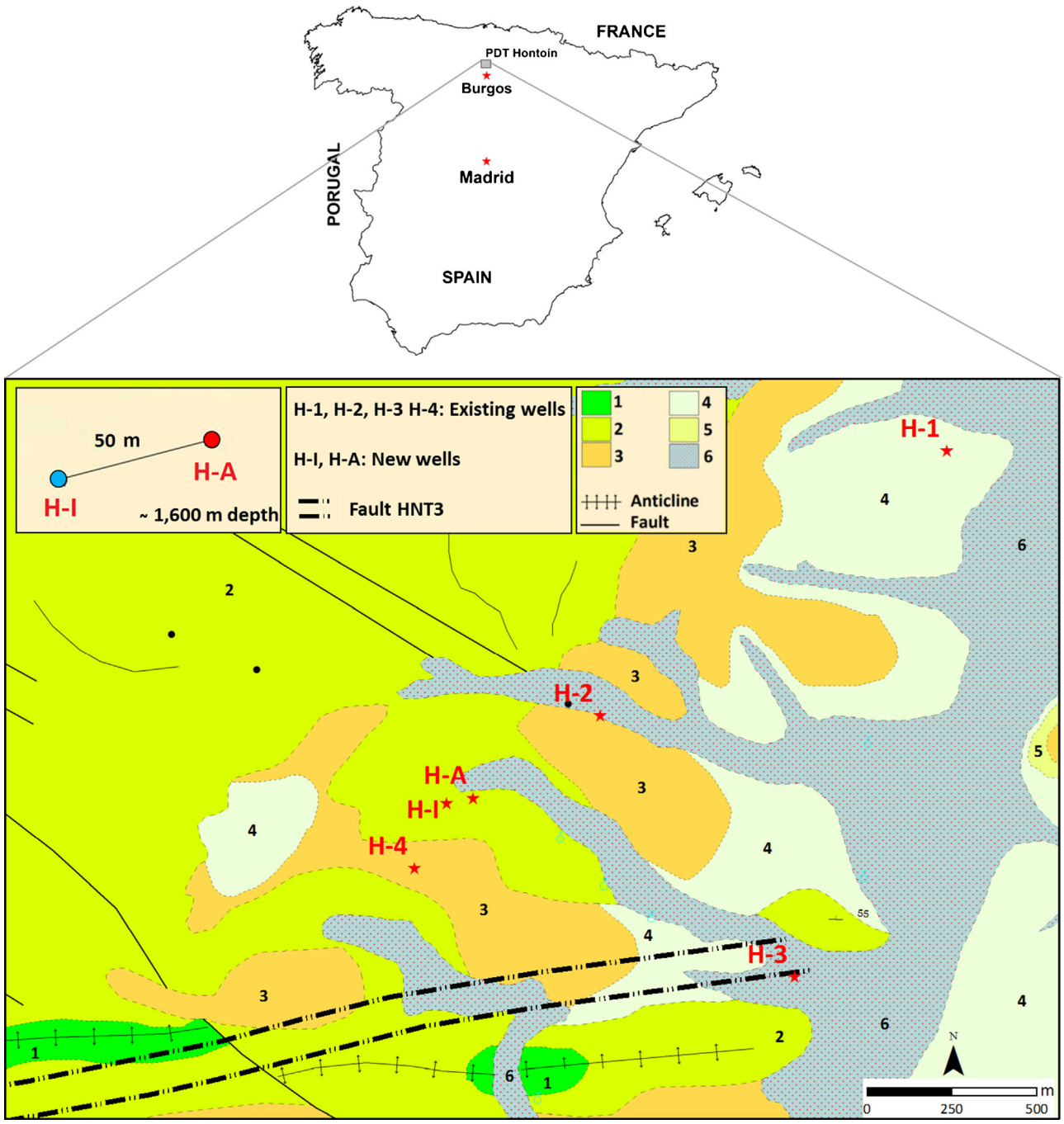

Fig. 1. Geological map of Hontomín area (IGME 1991) and location of the injection and monitoring wells. H-1 to H-4 are the pre-existing oil wells drilled in the eighties. Dotted lines refer to the approximate location of Fault HNT3, identify in the CIUDEN geological characterization ("south fault" Alcalde et al., 2013). 1. Mesozoic (marls, calcarenites and limestones); 2. Mesozoic (limestones and white dolomites); 3. Cenozoic (calcareous conglomerates and red clays, marginal Bureba Fm.); 4. Cenozoic (red clays with sand channels, sandstones and conglomerates, Bureba Fm.); 5. Cenozoic (alterations of red clay, with sand channels, limestones and marl (lake), and caliche, Carcedo Fm); 6. Quaternary deposits (gravels, and stones polygenic, sand, clay travertine and white marl, bed and lower valley).

the accumulation chamber, P [bar] is the atmospheric pressure, PM is the molecular weight of the gas (for $CO_2 = 44\,g\,mol^{-1}$), R is the constant of the ideal gases ($0.08314510\,bar\,l\,K^{-1}\,mol^{-1}$) and T [K] is the air temperature.

From October 2009 to April 2011, twelve sampling campaigns were carried out in the Hontomin site by analyzing more than 4000 CO_2 soil flux measurements. All the sampling campaigns were included within a circular area of about 6 km in diameter whose center was the H-2 well (Fig. 2). The number of measurements in the campaigns ranges from 30 (C-0) to 1102 (C-5). The CO_2 flux measurements were carried out all the year round to verify the effects caused by seasonal variability and rainfalls. Temperature and rainfall variations on a monthly basis for the period of observation are reported in Fig. 3 (data are from the meteorological station of Hontomín: http://meteo-hontomin.net). Climate at Hontomín is characterized by a continental regime with hot and dry summers, and cold winters. The highest temperatures and lowest rainfalls are indeed recorded at the end of spring and summer, whereas in December temperatures are around 0 °C and rainfalls reach the highest values. Snow is relatively frequent in January and February, although no data are available in this respect. These climatic conditions affect the contribution to the soil CO_2 by the biological

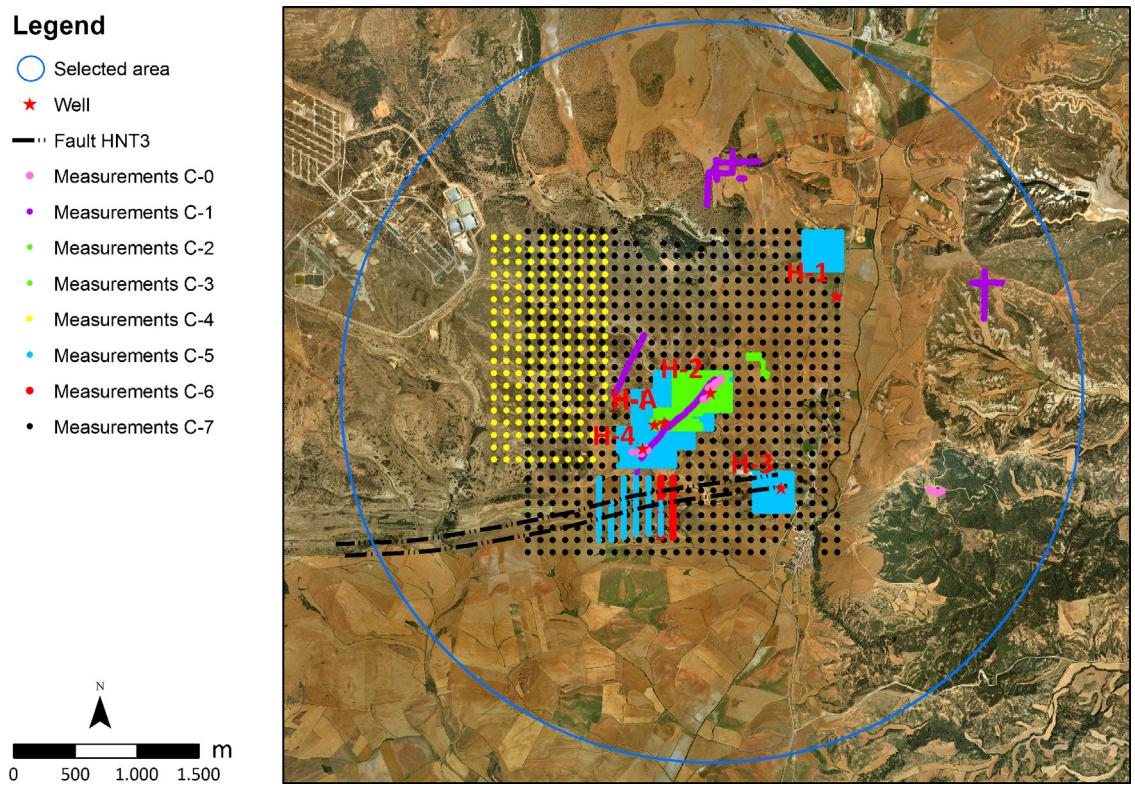

Fig. 2. Aerial view of the Hontomín area and location of the CO_2 flux campaigns (see also Tables 1 and 2). Dotted lines indicate the approximate location of Fault HNT3 ("south fault", Alcalde et al., 2013).

activity that achieves its climax in summer, while in winter it is minimal.

The first two campaigns (namely C-0 and C-1, Table 1) were aimed to assess a measurement protocol and an appropriate geostatistic approach, while the CO_2 flux measurements carried out in January (C-1.1), February (C-1.2) and March (C-1.3) 2010 were used to validate the protocol (Elío et al., 2012). As reported in Elío et al. (2012), the protocol was including the following steps: (1) cleaning and removal of both the vegetal cover and the very first layer (about 2 cm) of the soil, (2) waiting (about 1 h) to prevent flux perturbation due to the soil removal and (3) measuring the CO_2 flux. The results from these two campaigns were used for the successive measurements to assess (i) the seasonal variability of CO_2 soil flux, (ii) evaluate the CO_2 output and (iii) define a CO_2 geochemical baseline.

Geostatistical analyses showed that at Hontomín the maximum distance for which a spatial autocorrelation exists for the CO_2 flux was about 110 m. This value was then used to establish the appropriate distance between consecutive sampling points. For the geochemical baseline, two distinct strategies were followed:

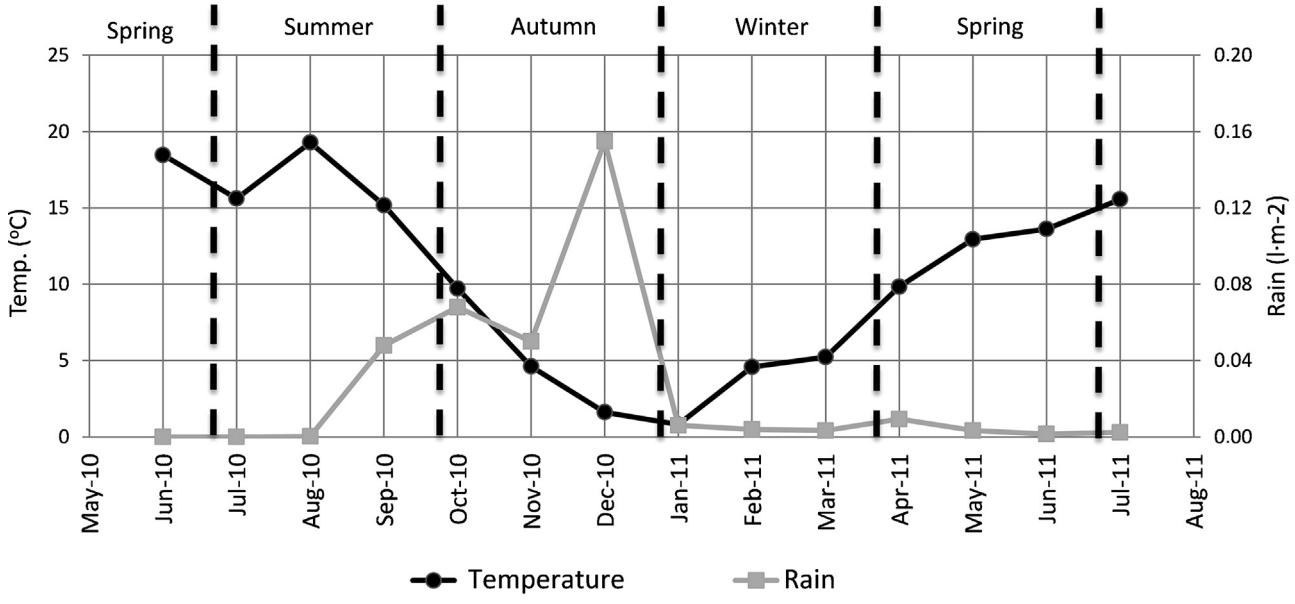

Fig. 3. Temperature and rain (monthly averages) from June 2010 to July 2011 at the Hontomín meteorological station.

Table 1
Summary of the CO_2 flux statistical methodology campaigns at Hontomín.

	C-0	C-1	C-1.1	C-1.2	C-1.3
Date	October 2009	November 2009	January 2010	February 2010	March 2010
Number of points measured	30	768	230	55	116
Aims	Recognition of the sampling zone Orientative measurements with the accumulation chamber	Establishment of the measurement protocol Geostatistical analysis	Validation of the protocol of the measurement of the CO_2 flux Establishment of the measurement protocol and maximum scopes for carrying out the sampling campaigns		
		Measurements according to four zones	Comparison among 3 measurement strategies		
Minimum value of CO_2 ($g\,m^{-2}\,day^{-1}$)	1.40	0.51	<LD	<LD	1.36
Average value of CO_2 ($g\,m^{-2}\,day^{-1}$)	10.42	9.12	2.023	3.48	6.29
Maximum value of CO_2 ($g\,m^{-2}\,day^{-1}$)	32.30	81.07	27.97	28.80	18.85
Standard deviation	7.18	6.04	2.58	4.54	3.63

(i) large-scale grids (100 m) (namely C-4: area 1.90 km^2 and C-7: area 7.02 km^2) and (b) small-scale (25–30 m) grids in those sites adjacent to both the existing oil boreholes and those where the H-I and H-A wells will be drilled (C-2, C-3, C-5, C-6) and across the HNT3 fault (Fig. 2). A summary of main features of the baseline CO_2 soil flux campaigns along with the minimum, maximum and average values is reported in Table 2.

In all campaigns CO_2 soil flux measurements were repeatedly carried out to test the reproducibility and the repeatability of the data. Additionally, in each site meteorological parameters such as pressure, temperature, relative humidity and wind speed were measured.

For the C-2 to C-7 campaigns CO_2 contour maps were drawn. The output of CO_2 for each sampling campaign was estimated by sequential Gaussian simulations (sGs) (Lewicki et al., 2005). Predictions and simulations were carried by ordinary kriging after a normal transformation of the data, applying a trans-Gaussian kriging with Box–Cox transformation. The Box-Cox transformation of data (X) with the transformation parameters lambda (λ) is (Box and Cox, 1964):

$$\phi_{\lambda}^{-1}(X) = \begin{cases} \dfrac{X^{\lambda}-1}{\lambda} & \lambda \neq 0 \\ \log(X) & \lambda = 0 \end{cases}$$

The trans-Gaussian kriging predictor of $Y(s_o)$ is (Pebesma, 2004 and references therein):

$$\widehat{Y}(s_o) = \phi(\widehat{Z}(s_o)) + \phi''(\widehat{\mu})\left(\frac{\sigma_k^2(s_o)}{2} - m\right)$$

$$\phi(x) = \begin{cases} (x\cdot\lambda+1)^{1/\lambda} & \lambda \neq 0 \\ e^{x} & \lambda = 0 \end{cases}$$

$$\phi''(x) = \begin{cases} \left(\dfrac{1}{\lambda}-1\right)\cdot\lambda\cdot(x\cdot\lambda+1)^{\left(\frac{1}{\lambda}-2\right)} & \lambda \neq 0 \\ e^{x} & \lambda = 0 \end{cases}$$

where $\hat{Z}(s_o)$ is the ordinary kriging predictor on the transformed scale data, $\sigma^2{}_k(s_o)$ the ordinary kriging variance, $\hat{\mu}$ the mean estimate at each location and m the Lagrange parameter for each location.

It is remarkable that the C-5 campaign, in the vicinity of the H-1 and H-3 oil wells (Table 1; Fig. 2), the experimental variograms are within envelop of all those variograms, obtained after randomly permuting the coordinates data. Thus, no spatial relationships exist among the data and geostatistic analysis is not an adequate prediction method. As a consequence, the interpolation method selected for predicting the CO_2 flux is the Local Polynomial Regression Fitting (function "loess", of "R" program; R Core Team, 2012; Cleveland et al., 1992). The total emission, i.e. output, of CO_2, for each area where the CO_2 fluxes were measured, was calculated by Sichel estimation (Chiodini et al., 1998; Lewicki et al., 2005).

4. Results and discussion

The CO_2 flux values at Hontomín had average values ranging between 4.9 and 13 $g\,m^{-2}\,d^{-1}$, although most were below

Table 2
Summary of the CO_2 flux baseline campaigns at Hontomin.

	C-2	C-3	C-4	C-5	C-6	C-7
Date	May 2010 (Spring)	July 2010 (Summer)	October 2010 (Autumn)	March 2011 (Winter)	March 2011 (Winter)	April 2011 (Spring)
Number of points measured	316	303	233	1102	43	816
Aims	Establishing of the baseline of the CO_2 flux					
	Control in the vicinity of the test drill H-2	Control in the vicinity of the test drills H-2	Control in the zone of the future positioning of the injection test drill	Control close to the test drills H-1, H-2, H-3 and H-4 and the zone of the fault HNT3	Control of the fault HNT3	Control of the injection zone
	Grid 30 m × 30 m	Grid 30 m × 30 m	Grid 100 m × 100 m	Grid 30 m × 30 m	Profiles orthogonal to the fault HNT3	Grid 100 m × 100 m
Minimum value of CO_2 ($g\,m^{-2}\,day^{-1}$)	0.11	0.08	0.62	0.03	0.16	0.15
Average value of CO_2 ($g\,m^{-2}\,day^{-1}$)	8.54	11.04	4.87	5.46	4.99	13.04
Maximum value of CO_2 ($g\,m^{-2}\,day^{-1}$)	45.90	39.61	29.46	60.89	27.01	58.38
Standard deviation	6.04	7.15	2.95	5.89	4.35	8.12

Table 3
CO_2 soil degassing values from hydrothermal, volcanic and CCS areas. CO_2 fluxes in Mediterranean ecosystems are reported for comparison.

Site		Range CO_2 flux ($g\,m^{-2}\,d^{-1}$)	Range Mean CO_2 flux ($g\,m^{-2}\,d^{-1}$)	References
Natural Analogs	"La Sima" Campo de Calatrava, Spain	1000–13,700	–	Elío et al. (unpublished)
	"Jabalón" Campo de Calatrava, Spain	600–5000	–	
	"Solfatara" Phlegrean Fields, Italy	75–23,200	–	
	Active volcanoes	0.11–<297,000	–	Möner and Etiope (2002)
	Geothermal or active tectonic zones	0–32,600	–	
CCS Projects	Compostilla OXYCFB300 (Hontomin, Castilla y León, Spain) (Saline aquifer)	0.03–60.89	4.87–13.04	Mazadiego et al. (2012)
	Rangely CO_2-EOR project (Colorado – EE.UU.) (EOR)	–	0.33–3.80	Klusman (2003b)
	Teapot Dome (Wyoming – EE.UU.) (EOR)	−0.3–0.73	0.23	Klusman (2005)
	CO_2SINK Project (Ketzin – Alemania) (Saline aquifer)	–	2.00–19.00	Förster et al. (2006)
Soil respiration				
Normal biologic fluxes Temperate climate fields		–	1.64–9.59	Möner and Etiope (2002)
Global mean flux		–	1.8	
Annual soil respiration rates: coniferous, temperate grassland, Mediterranean Woods, etc.		–	0.02–7.10	Raich and Schlesinger (1992)
Farming areas Castilla y León (Spain)		0.76–30.40	3.40–13.30	Sánchez et al. (2003)
Mean monthly soil respiration in Mediterranean ecosystem	Forest	–	4.20–17.90	Almagro et al. (2009)
	Abandoned field	–	2.15–13.60	
	Olive grove	–	4.20–12.50	

$20\,g\,m^{-2}\,d^{-1}$. Minimum values were from 0.03 (C-5) to 0.62 (C-4) $g\,m^{-2}\,d^{-1}$, while the maximum ones ranged from 27.01 (C-6) to 60.89 (C-5) $g\,m^{-2}\,d^{-1}$. The recorded CO_2 values at Hontomín were within the ranges observed in other Mediterranean ecosystems where CO_2 is mainly sourced by biological respiration and in agreement with other data obtained in other CCS projects (Table 3). When compared to CO_2 natural analogs from volcanic and geothermal areas, the Hontomín soil fluxes are indeed several orders of magnitude lower (Table 3). This suggests that no deep CO_2 inputs (e.g., residual hydrocarbons deposit or thermometamorphic and mantle CO_2) appear to contribute to the soil gas emission and soil respiration is the only responsible for the observed CO_2 flux at Hontomín. To further corroborate this assessment, Nisi et al. (2013) reported highly negative $\delta^{13}C$-CO_2 (as low as −23‰ PDB) values in spring waters from Hontomín and surrounding areas.

Histograms and probability curves of CO_2 flux values are reported in Fig. 4; data for the C-0 to C-1.3 campaign measurements were not considered since they were used to standardize the measurement procedure. For the C-5 campaign, 4 sub-areas were considered and related to vicinity to the H-2 and H-4, H-1 and H-3 oil boreholes and a south fault HNT3 (Figs. 1 and 2). CO_2 fluxes are characterized by lognormal distributions for C-4, C-5 (H-1), C-5 (H-3) and C-5 (fault zones). Despite the fact that in the C-6 campaign a relatively low number of measurements were carried out, the CO_2 flux values may be referred to a lognormal distribution. The C-2, C-3, C-5 (H2/H4) and C-7 data show short-tail to the left of the histograms corresponding to low CO_2 flux (around $1\,g\,m^{-2}\,d^{-1}$). This produces an effect of a mixing between two lognormal populations that can be explained in terms of different land use, able to produce different, though low, CO_2 flux (see below) (Raich and Schlesinger, 1992; Almagro et al., 2009). Alternatively, CO_2 fluxes close the instrumental detection limit ($\approx 0.2\,g\,m^{-2}\,d^{-1}$) are affected by a greater error (up to 30%) and may produce the short-tails observed for some histograms (Fig. 4).

The C-2, C-3 and C-7 data are more dispersed, showing higher standard deviations (Table 2). These campaigns were carried out in warm periods (spring 2010, summer 2010 and spring 2011, respectively) when soil respiration is higher and the CO_2 fluxes become more heterogeneous due to several process in the soil (Sánchez et al., 2003).

4.1. Effect of land use

No significant differences in CO_2 flux were recorded in areas with different lithologies (Elío et al., 2012). In contrast, the vegetation effect (land use) appears to be significant. As a consequence, the area of Hontomín was divided into 4 main typologies of land use: (a) forest and (b) cultivated (mainly wheat or barley) at which (c) fallow and (d) ploughed terrains were added. In Table 4, the CO_2 fluxes, divided according to seasonal variability, are reported as a

Table 4
CO_2 flux values ($g\,m^{-2}\,d^{-1}$) at Hontomín according to the land use and seasonal variability.

	Minimum	Average	Maximum	*N*
Spring 2010				
Agricultural				
Ploughed	0.11	2.86	16.12	83
Fallow	–	–	–	–
Cultivated	3.27	8.68	14.36	6
Forest	0.52	10.82	45.90	207
Summer 2010				
Agricultural				
Ploughed	–	–	–	–
Fallow	1.30	8.87	27.14	25
Cultivated	0.75	8.37	39.61	38
Forest	0.08	11.75	37.39	220
Autumn 2010				
Agricultural				
Ploughed	–	–	–	–
Fallow	–	–	–	–
Cultivated	–	–	–	–
Forest	0.62	4.87	29.46	233
Winter 2011				
Agricultural				
Ploughed	–	–	–	–
Fallow	2.63	4.75	8.59	14
Cultivated	0.03	5.58	60.89	528
Forest	0.11	5.33	19	600
Spring 2011				
Agricultural				
Ploughed	0.90	6.19	33.94	26
Fallow	0.83	11.98	32.94	42
Cultivated	0.68	13.46	58.38	310
Forest	0.15	13.24	48.13	438

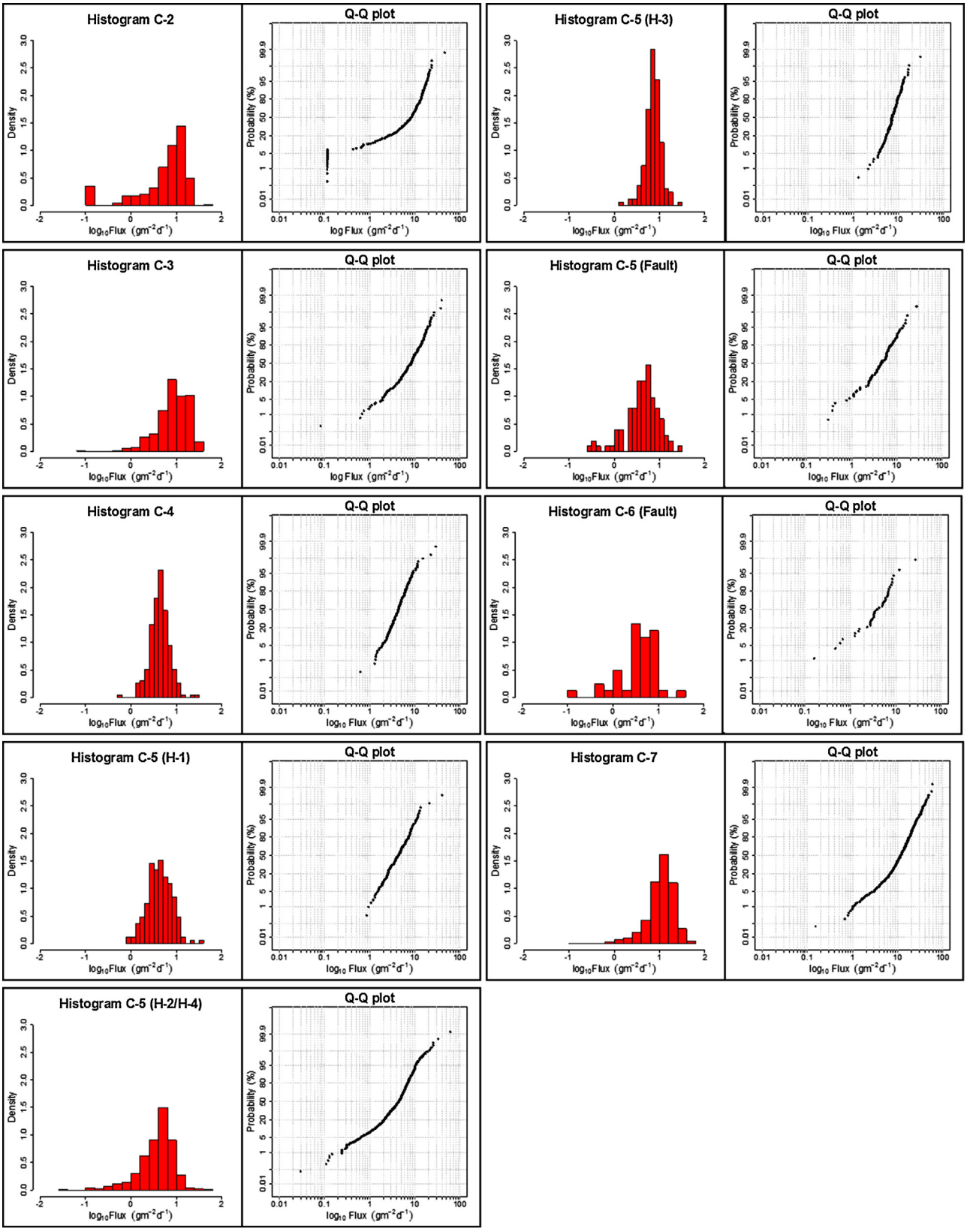

Fig. 4. Histograms and probability curves of the CO_2 flux values at Hontomín.

function of the land use. The CO_2 fluxes were varying significantly when the same season was taken into account. Cultivated areas showed the highest values, independently on the season. In order to better visualize whether the variations of the CO_2 fluxes were associated to the different land use and seasonal variability, CO_2 soil fluxes (as box-plot) are plotted versus time in Fig. 5 by distinguishing the different usages of the land. Ploughed lands had the lowest CO_2 flux values. Forests, fallow and cultivated lands displayed a

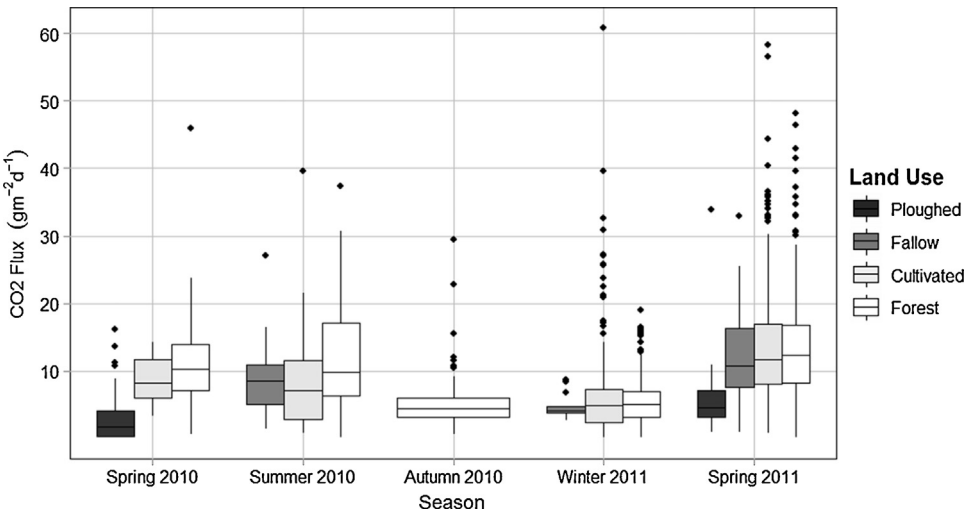

Fig. 5. Box-plot of the CO_2 soil flux versus time.

larger variability and seem more strongly affected by seasonality. A slight increase in CO_2 flux was observed during the warmer periods (spring-summer, with the highest values in spring 2011), likely related to a higher biological activity. On the other hand, the lowest values were observed in autumn and winter.

The influence of land use can also be observed in the contour maps drawn for campaigns C-2 (Fig. 6), C-5 (Fig. 7) and C-7 (Fig. 8). In campaign C-2 (Fig. 6) a clear drop in the CO_2 flux was recorded when the soil was ploughed (circle points). In C-7 (Fig. 8), despite the few measurements in ploughed areas, the CO_2 fluxes values were usually lower than those measured in non-ploughed areas. In general, no significant differences were observed when comparing CO_2 fluxes from cultivated agricultural and fallow soils with respect to those from forested soils.

Plough operations are expected to increase soil aeration, thus enhancing soil respiration and as a consequence, CO_2 flux. Nevertheless, our data show a clear drop in the CO_2 flux. This can mainly be due to dilution process by air, favored by the strong winds that affect Hontomín (frequently N-S directions up to 5 m s^{-1}, with maximum values up to 26 m s^{-1}, http://meteo-hontomin.net), since plough produces an exponential increase of the porosity in the superficial layers of the soil. The absence of vegetation in ploughed areas may also represent an important factor as a diminished contribution to the total soil CO_2 flux is expected by root respiration.

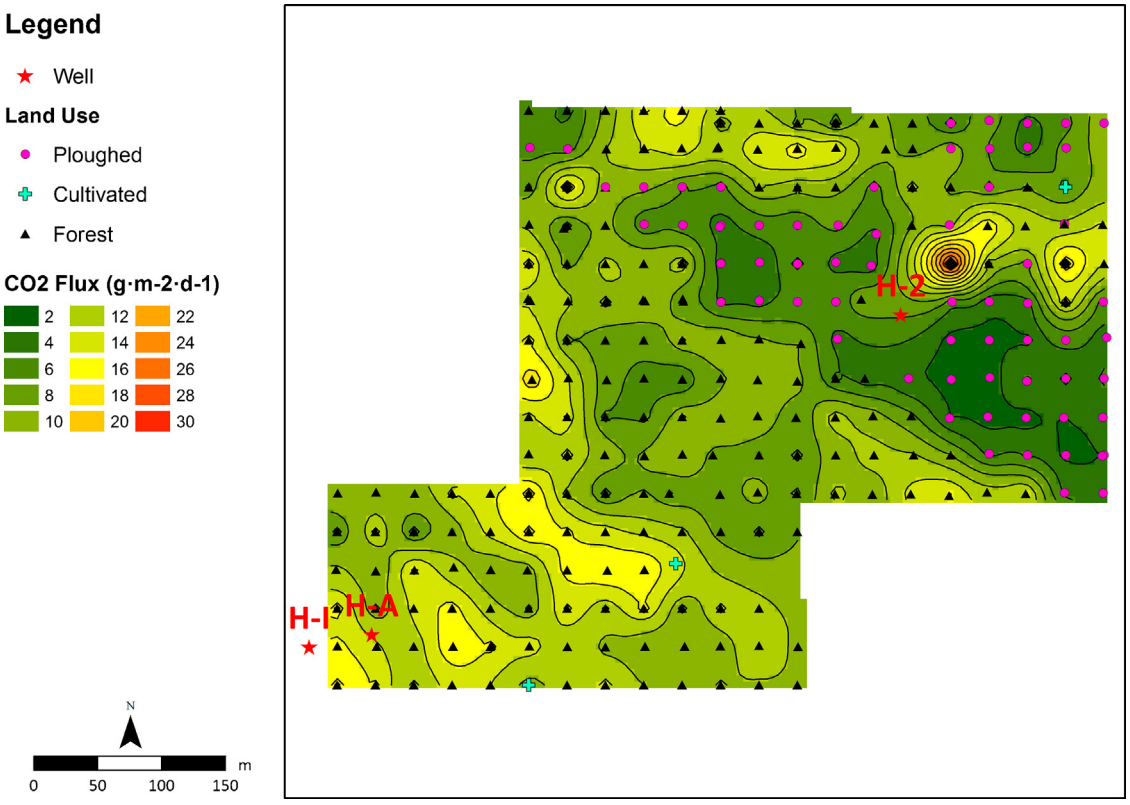

Fig. 6. CO_2 flux contour map for campaign C-2 (small scale). Sites of measurements are reported with different colors as a function of the land use.

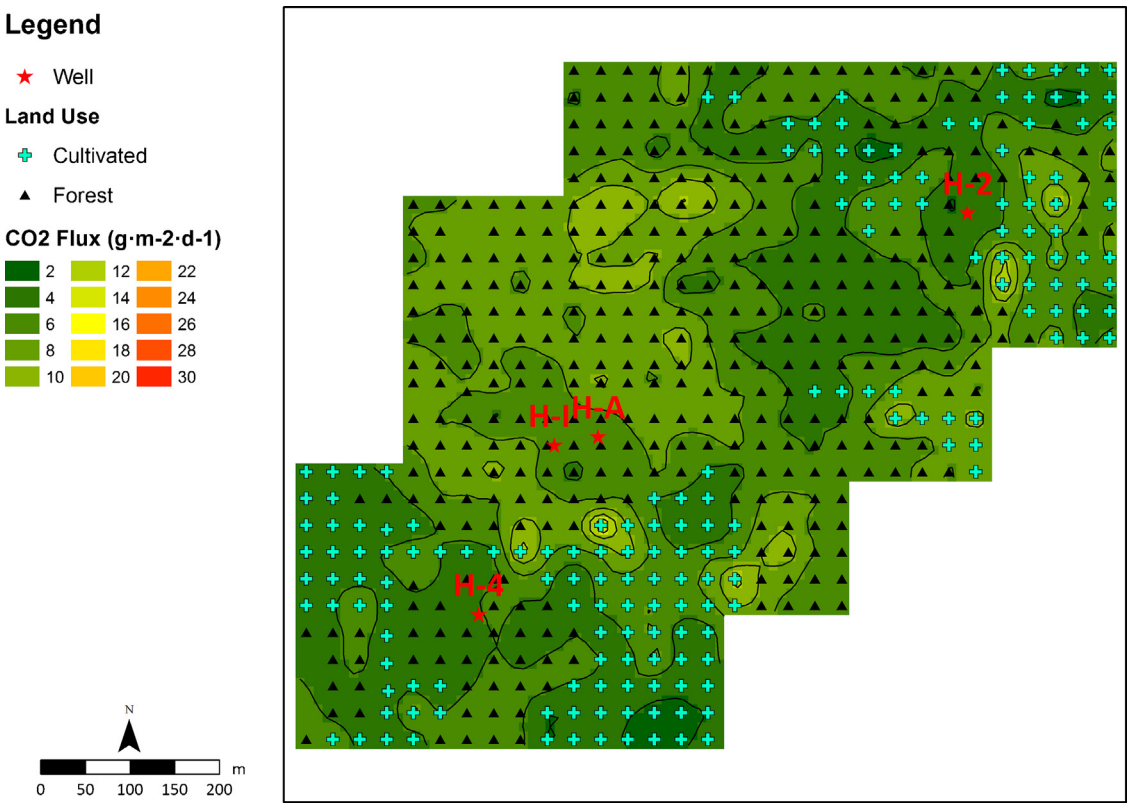

Fig. 7. CO_2 flux contour map for campaign C-5 (small scale). Sites of measurements are reported with different colors as a function of the land use.

4.2. CO_2 fluxes in the vicinity of deep faults

An interesting point of the baseline studies at Hontomín was the detection of a potential outflow of fluids from deep reservoirs through the fault zone located in the south of the pilot plant. In this area, magnetotelluric 2D characterization suggests an important fluid circulation along this fracture (Ogaya et al., 2013), in agreement with the geochemical data from some springs in the area, which indicate a possible contribution by deep waters (e.g. springs at Fuente de Hontomín and Fuente Laguillo; Nisi et al., 2013). To check the potential enhanced gas flux, diffuse soil CO_2 measurements perpendicular to the fault strike were performed following

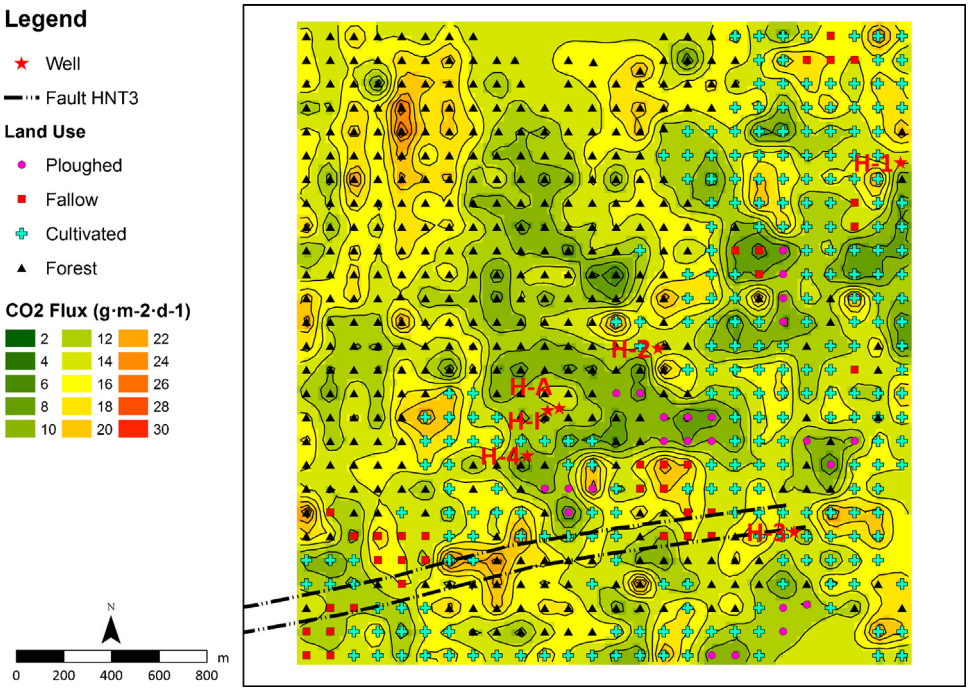

Fig. 8. CO_2 flux contour map for campaign C-7 (large scale). Sites of measurements are reported with different colors as a function of the land use.

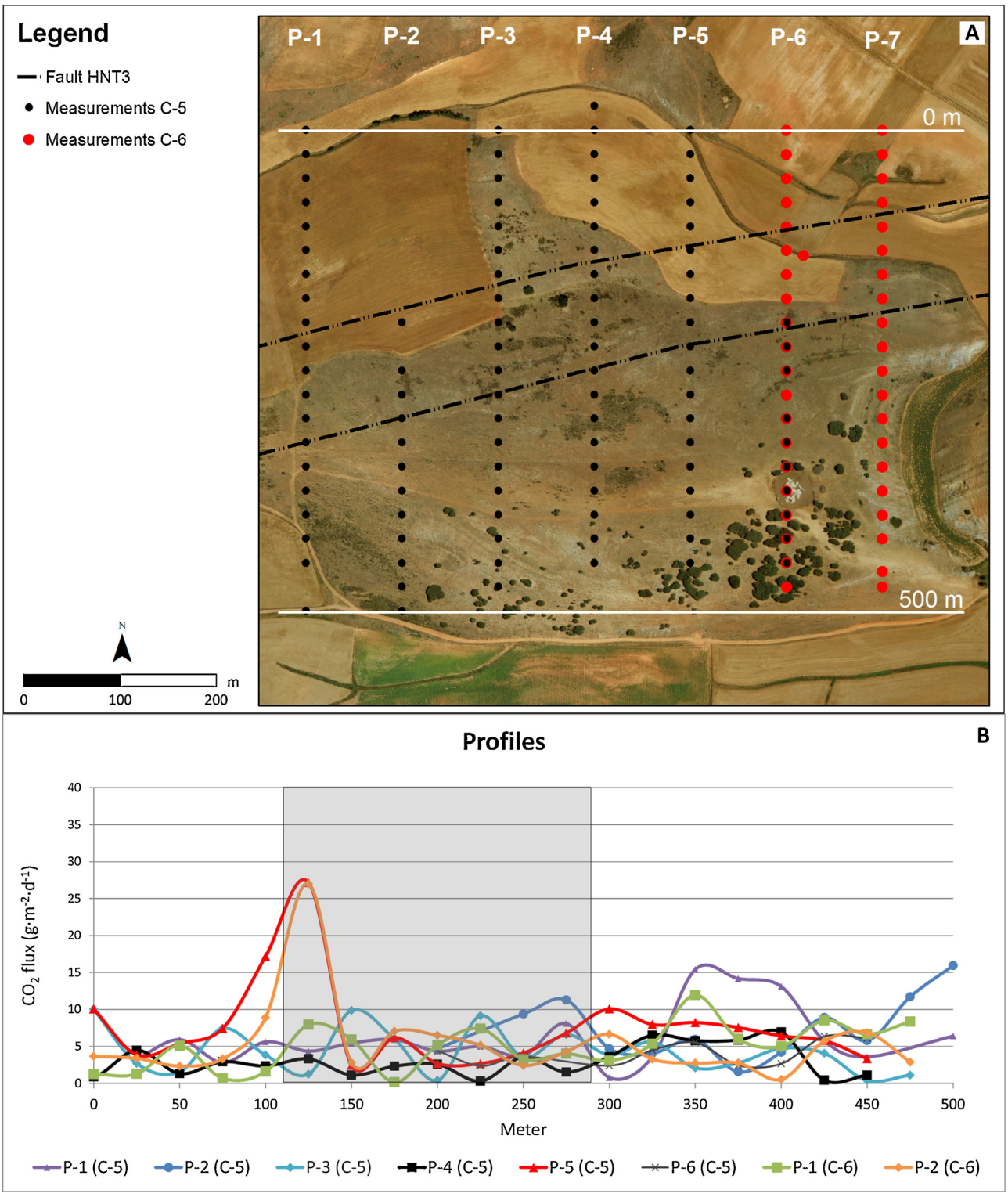

Fig. 9. Soil diffuse CO_2 measurement sites across the HNT3 fault system (Fig. 9a) and CO_2 flux values (Fig. 9b) through the faulted are (gray area).

profiles perpendicular to, with 100 m of separation between them and with distances of 25 m between measurement stations (Fig. 9a). No significant increases in the CO_2 flux were observed, their values being included between <0.01 and 27 g m^{-2} d^{-1} (Fig. 9b), with an average value of 5 g m^{-2} d^{-1} and thus, similar to undisturbed areas.

4.3. CO_2 flux at Hontomín area

Contour maps of Figs. 7 and 8 for small-scale (C-5: close to the H-2 and H-4 oil boreholes) and large-scale (C-7: distributed throughout the whole area) campaigns, carried out in March and April 2011, respectively, indicate that in the first case, CO_2 fluxes

Table 5
Area (in km^2), CO_2 output (in ton d^{-1}) and mean estimation (in ton km^{-2} d^{-1}) at Hontomín.

Campaign		Area (km^2)	Mean estimation (ton km^{-2} d^{-1})	CO_2 emission rate (ton d^{-1})		
				Emission	Confidence intervals (95%)	
C-2		0.198	8.56	1.7	1.6	1.8
C-3		0.198	9.25	1.8	1.7	1.9
C-4		1.900	4.74	9.0	8.4	9.6
C-5	H-2/H-4	0.495	4.98	2.5	2.3	2.6
	H-1	0.106	5.14	0.54	0.49	0.60
	H-3	0.106	7.87	0.83	0.78	0.88
C-7		7.020	13.14	92	89	95

are low and homogeneous. Apparently, no influence by the oil wells was recognized, i.e. no leakage is apparently present by the boreholes. CO_2 fluxes for C-7 campaign are slightly higher and more heterogeneously distributed (Fig. 8). Nevertheless, the relatively high values do not seem to be associated with any geological structure or CO_2 migration pathways, i.e. no anomalous zones, possibly related to high permeability (fault) zones, were recognized. As a consequence, the increment in the CO_2 fluxes can be interpreted as related to the increase in the biological activity.

The total CO_2 outputs from the C-2 to C-7 campaigns are listed in Table 5. Data for the C-6 measurements were not included due to the small number of observations. The extension of each area is variable and ranges between 0.106 (C-5/H-1 and C-5/H3) and 7.020 (C-7) km^2. The emission rate of CO_2 (in ton d^{-1}) and the confidence intervals (95%) are between 0.54 ± 0.05 [C-5 (H-1)] and 92 ± 3 (C-7) (Table 5). As expected, the larger the surface the higher the CO_2 output. Nevertheless, C-5/H-1 and C-5/H-3 have the same surface but the latter has a CO_2 output (0.83 ton d^{-1}) that is about 40% higher than the former (0.54 ton d^{-1}). If the emissions are normalized to 1 km^2 (mean estimation in Table 5), the highest CO_2 outputs were measured for the C-7 campaign (13.14 ton km^{-2} d^{-1}) and C-3 and C-2, (9.25 and 8.56 ton km^{-2} d^{-1} respectively). The minimum values are recorded in C-4 (4.74 ton km^{-2} d^{-1}) and C-5 (from 4.98 to 7.87 ton km^{-2} d^{-1}). Considering the seasonal variability, the highest values (C-7, C-3 and C-2) correspond to warmer spring-summer periods and minimum (C-4 and C-5) to cold autumn-winter periods, likely corresponding to periods of different biological activity.

CO_2 outputs at Hontomín lie within the range of averaged CO_2 flux from biological activity in Mediterranean ecosystems (Table 3; Almagro et al., 2009; Sánchez et al., 2003). On the other hand, data from Hontomín show values much smaller than those observed in many natural analogs of CO_2 leakage, which have a total CO_2 output up to three orders of magnitude higher (Fig. 10).

4.4. Reference values CO_2 flux baseline

For the determination of a geochemical baseline of the CO_2 fluxes, it is important to provide a reference value that can be assumed as a threshold, which, if exceeded, may be indicative of a possible CO_2 leakage from the reservoir during intra- and

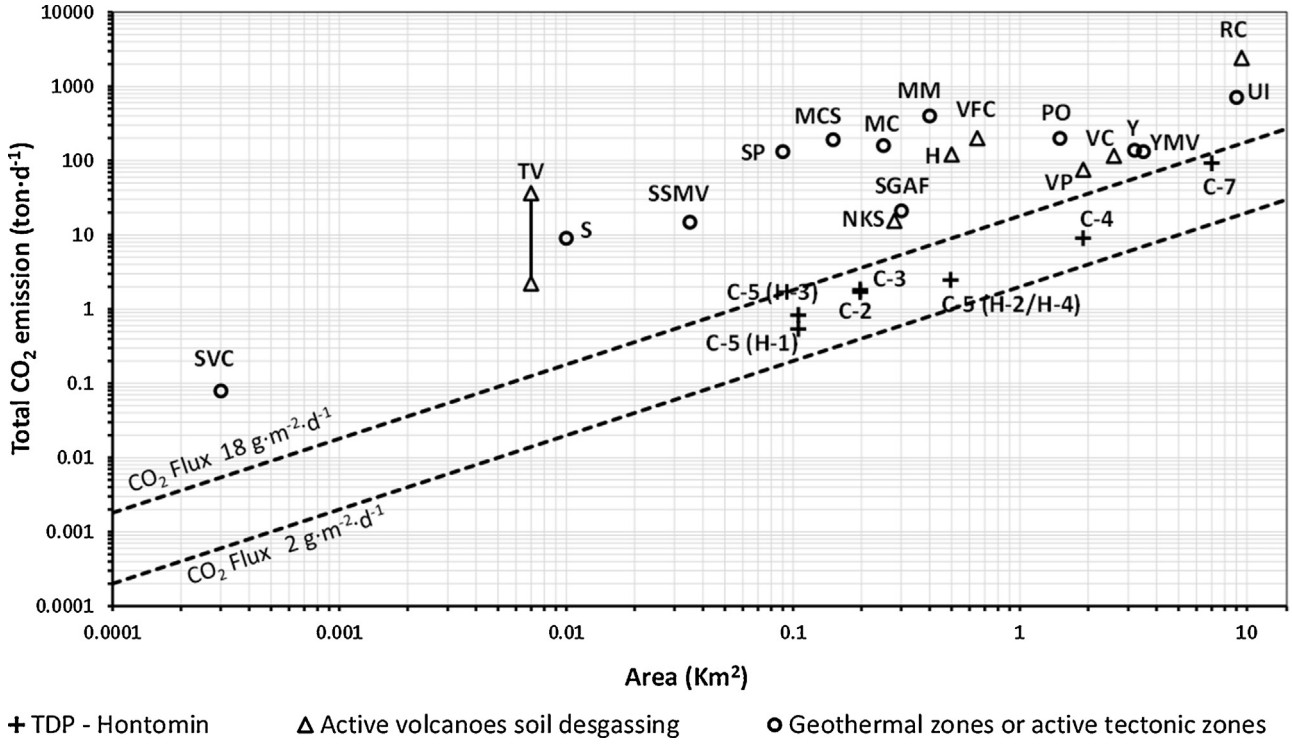

Fig. 10. CO_2 output rates for different areas (Möner and Etiope, 2002, and references therein) versus the total surface (in km^2). Dotted lines represent the maximum and minimum emission rate from averaged CO_2 flux from biological activity in Mediterranean ecosystems (see Table 3). H: Hakkoda (Japon), NKS: Nea Kameni Santorini (Greece), RC: Rabaul caldera (Papua N.G.), VC: Vulcano caldera (Italy), VFC: Vulcano Fossa crater (Italy), VP: Vulcano plains (Italy), MM: Mammoth Mount. (California), MC: Manziana Caldara (Italy), MCS: Manziana Caldara-Solfat. (Italy), PO: Poggio Olivo (Italy), SSMV: Salton Sea Mud V. (California), SVC: San Vincenzo la Costa (Italy), S: Selvena (Italy), SGAF: Siena G. Arbia Fault, SP: Solfatara, Phlegrean Fields (Italy), UI: Ustica Island (Italy), Y: Yangbajain (Tibet), YMV: Yellowstone Mud Volcano (Wyoming), TV: Teide Volcano (Spain) (output range, period 1999–2010, Melián et al., 2012).

Table 6
Reference values and confidence intervals (95%) of CO_2 flux (in $g\,m^{-2}\,d^{-1}$).

Season	Land use	No data	Percentile 50	Percentile 99
Autumn winter	Ploughed	0	n.d.	n.d.
	Fallow cultivated forest	1375	4.8 (4.5–5.0)	20 (16–26)
Spring summer	Ploughed	109	2.5 (1.7–3.5)	16 (11–34)
	Fallow cultivated forest	1286	11 (10–12)	37 (33–42)

post-injection operations. However, as previously mentioned, CO_2 fluxes are affected by weather conditions and land use. As a consequence, a single reference value cannot be considered representative of this threshold. At Hontomín (Fig. 5) two groups related to seasonal variations, autumn-winter and spring-summer, were recognized and in these groups CO_2 fluxes differentiate ploughed soil and the rest of land use (fallow, cultivated and forest). Thus, four references values have to be estimated.

Reference values are calculated as the 50th and 99th percentile using bootstrap resampling with all data of the different four groups, as outliers values were not observed (Table 6; Davison and Hinkley, 1997; Canty and Ripley, 2012). These results should be interpreted as an interval for which when percentile and confidence values of the CO_2 flux measurement are higher and not included in the reference confidence range of their respective groups, it could reasonably be supposed that a leakage from the CO_2 reservoir is occurring. Utilization of percentiles, instead of the arithmetical mean, is due to the fact that a robust measure of the values of CO_2 flux population has to be considered and moreover, they are less influenced by anomalous values. These percentiles are good indicators of CO_2 flux changes and once exceeded, the area should supposedly be monitored more frequently in order to define the area where the CO_2 is occurring.

Exceeding the estimated 99th percentile upper confidence limit (UCL_{99}) an evidence of leakage can seriously be considered. In our case $26\,g\,m^{-2}\,d^{-1}$ of CO_2 for autumn–winter in not-ploughed areas and 34 and $42\,g\,m^{-2}\,d^{-1}$ of CO_2 for spring–summer in ploughed and not-ploughed areas respectively. When the 50th percentile is considered, the presence of a CO_2 flux increase cannot unequivocally be related to deep leakage; consequently, an increment by the biological activity cannot be ruled out. Thus, the calculated 50th percentile upper confidence limit (UCL_{50}) of $5\,g\,m^{-2}\,d^{-1}$ for non-ploughed areas in autumn–winter season and 3.5 and $12\,g\,m^{-2}\,d^{-1}$ for ploughed and non-ploughed areas in spring–summer season, respectively, is in accordance with the mean average CO_2 flux in Mediterranean ecosystems (Table 3; Almagro et al., 2009; Sánchez et al., 2003). Values of $18\,g\,m^{-2}\,d^{-1}$ could then be referred to an indicator of average of biological CO_2 flux measurements and they have to be in consideration when CCS monitoring will be carried out.

5. Conclusions

Background CO_2 fluxes in the soil–atmosphere interface in the Hontomín area when the TDP on CO_2 Storage is under construction and will probably be finished at the end of 2013 in the framework of the Compostilla OXYCFB300 project are low and typical of biological respiration. The average values were between 4.9 and $13\,g\,m^{-2}\,day^{-1}$, smaller than $18\,g\,m^{-2}\,d^{-1}$, which may be considered as an upper limit of the arithmetical mean for soil respiration CO_2. Evidences of deep CO_2 inputs (e.g. residual hydrocarbons deposit) were not detected, suggesting that the soil respiration is the only responsible for the observed CO_2 flux at Hontomín.

Measurements were also carried out in zones of preferential ascent of deep fluids, i.e. in the vicinity of (i) oil wells (H-1, H-2, H-3 and H-4), (ii) ongoing injection and monitoring wells (H-A and H-I) and (iii) fault zones (HNT3). The CO_2 soil fluxes in all these areas were very similar to those recorded in undisturbed zones. Only few anomalies (around $40\,g\,m^{-2}\,d^{-1}$) near the H-2 oil well were detected. These values cannot be associated to a deep source of CO_2 and it is likely that they are due to an increase in the biological activity. Nevertheless, this zone should be regarded as a potential risk area for leakages during and after the CO_2 injection.

Slightly higher values of the CO_2 flux values were observed during warmer periods as the biological activity increases. In a similar way, CO_2 flux was higher in areas where vegetated (cultivated and forestry) areas dominated.

At Hontomín, CO_2 flux is low and homogenously distributed in winter, whereas in warms periods it is heterogeneous and higher due to the increased biologic activity. Thus, the detection of possible leakages from the reservoir in CCS projects can more easily be recognized in autumn–winter, during which the "noise" from biologic activity is strongly reduced with respect to that occurring in spring–summer time.

The determination of reference CO_2 flux values above which a possible leakage from the reservoir can be considered realistic may help in monitoring and verification programs during CCS projects. Two groups of CO_2 flux values were then calculated. The first ones (UCL_{50}, $5\,g\,m^{-2}\,d^{-1}$) can be referred to non-ploughed areas in autumn–winter and 3.5 and $12\,g\,m^{-2}\,d^{-1}$ for ploughed and non-ploughed areas in spring-summer time. These values can be used as an indicator of an increasing CO_2 flux and as a warning of possible early leakage. If these values are exceeded, monitoring programs have to be more exhaustive and frequent to evaluate the evolution of a possible early leakage and associated risks. The second ones are for UCL_{99} of $26\,g\,m^{-2}\,d^{-1}$ during autumn–winter in not-ploughed areas and 34 and $42\,g\,m^{-2}\,d^{-1}$ for spring–summer in ploughed and not-ploughed areas respectively. Exceeding the estimated 99th percentile upper confidence limit an evidence of leakage can seriously be considered.

Soil CO_2 flux measurements in injection plants are a powerful tool to recognize CO_2 leakage at near surface and verify the feasibility of the safe storage of the greenhouse gas underground (Klusman et al., 2000; Klusman, 2003a; 2003b; 2005). However, prior the injection the geochemical baseline of the CO_2 fluxes is required to establish threshold fluxes to be used as reference values for the forthcoming campaigns as those defined for the Hontomín site.

Acknowledgements

This work has been financed by the Ciudad de la Energía Foundation, through the ALM-08-006 contract, and co-financed by the European Union (European Energy Program for Recovery). The sole responsibility of this publication lies with the authors. The European Union is not responsible for any use that may be made of the information contained therein. J. Elío was supported by the mobility program "Ayudas del Consejo Social de la Universidad Politécnica de Madrid para la Internacionalización de Doctorandos para el curso 2012-2013, (XI Convocatoria)," of the Social Council at the Technical University of Madrid.

References

Albanese, S., De Vivo, B., Lima, A., Cicchella, D., 2007. Geochemical background and baseline values of toxic elements in stream sediments of Campania region (Italy). Journal of Geochemical Exploration 93, 21–34.

Alcalde, J., Martí, D., Calahorrano, A., Marzan, I., Ayarza, P., Carbonell, R., Juhlin, C., Pérez-Estaún, A., 2013. Active Seismic Characterization Experiments of the Hontomín Research Facility for geological storage of CO_2. International Journal of Greenhouse Gas Control, Spain, http://dx.doi.org/10.1016/j.ijggc.2013.01.039.

Almagro, M., López, J., Querejeta, I., Martinez-Mena, M., 2009. Temperature dependence of soil CO_2 efflux is strongly modulated by seasonal patterns of moisture availability in a Mediterranean ecosystem. Soil Biology and Biochemistry 41, 594–605.

Arts, R., Winthaeoen, P., 2005. Monitoring options for CO_2 storage. In: Thomas, D., Benson, S. (Eds.), Carbon Dioxide Capture for Storage in Deep Geologic Formations – Results from the CO_2 Capture Project, 2. Lawrence Berkeley Laboratory, Berkeley, CA, USA, pp. 1001–1014.

Beaubien, S.E., Jones, D.G., Gal, F., Barkwith, A.K.A.P., Braibant, G., Baubron, J.-C., Ciotoli, G., Graziani, S., Lister, T.R., Lombardi, S., Michel, K., Quattrocchi, F., Strutt, M.H., 2013. Monitoring of near-surface gas geochemistry at the Weyburn, Canada, CO_2-EOR site, 2001–2011. International Journal of Greenhouse Gas Control, http://dx.doi.org/10.1016/j.ijggc.2013.01.013.

Box, G.E.P., Cox, D.R., 1964. An analysis of transformations. Journal of the Royal Statistical Society. Series B (Methodological) 26, 211–251.

Buil, B., Gómez, P., Peña, J., Garralón, A., Galarza, C., Durán, J.M., Domínguez, R., Escribano, A., Turrero, M.J., Robredo, L.M., Sánchez, L., 2012. Caracterización y monitorización hidrogeoquímica de los acuíferos superiores a la formación almacenamiento de CO2 (Hontomín, Burgos) y actualización de la caracterización de aguas superficiales. Informe técnico CIEMAT/DMA/2G010/1/2012 (in Spanish).

Canty, A., Ripley, B., 2012. Boot: Bootstrap R (S-Plus) Functions. R package version 1., pp. 3–7.

Cardellini, C., Chiodini, G., Frondini, F., 2003. Application of stochastic simulation to CO_2 flux from soil: mapping and quantification of gas release. Journal of Geophysical Research 108, 2425.

Cleveland, W.S., Grosse, E., Shyu, W.M., 1992. Local regression models. In: Chambers, J.M., Hastie, T.J. (Eds.), Statistical Models in S. Wadsworth and Brooks/Cole, Pacific Grove, pp. 309–376 (Chapter 8).

Chiodini, G., Cioni, R., Guidi, M., Raco, B., Marini, L., 1998. Soil CO_2 flux measurements in volcanic and geothermal areas. Applied Geochemistry 13, 543–552.

Cicchella, D., De Vivo, B., Lima, A., 2005. Background and baseline concentration values of elements harmful to human health in the volcanic soils of the metropolitan and provincial area of Napoli (Italy). Geochemistry: Exploration-Environment-Analysis 5, 29–40.

Davison, A.C., Hinkley, D.V., 1997. Bootstrap Methods and Their Applications. Cambridge University Press, Cambridge, ISBN 0-521-57391-2.

Elío, J., Ortega, M.F., Chacón, E., Mazadiego, L.F., Grandia, F., 2012. Sampling strategies using the accumulation chamber for monitoring geological storage of CO_2. International Journal of Greenhouse Gas Control 9, 303–311.

Frattini, P., Lima, A., De Vivo, B., Cicchela, D., Albanese, S., 2006. Atlante geochimicoambientale dei suoli dell'Isola d'Ischia. Aracne Editrice, Rome, Italy, ISBN 88-548-0818-0, pp. 244 pp.

Förster, A., Norden, B., Zinck-Jørgensen, K., Frykman, P., Kulenkampff, J., Spangenberg, E., Erzinger, J., Zimmer, M., Kopp, J., Borm, G., Juhlin, C., Cosma, C.G., Hurte, S., 2006. Baseline characterization of the CO_2SINK geological storage site at Ketzin, German. Environmental Geoscience 13, 145–161.

IEA Greenhouse Gas R&D, 2004. Inaugural Meeting of the Monitoring Network , November 8th–9th. Seymour Centre, University of California Santa Cruz, USA.

IGME 1991, Instituto Geológico y Minero de España. Mapa geológico de España, geological sheet 167/19-9 scale 1:50.000 Montorio.

IPCC, 2006. In: Eggleston, H.S., Buendia, L., Miwa, K., Ngara, T., Tanabe, K. (Eds.), 2006 IPCC Guidelines for National Greenhouse Gas Inventories. Prepared by the National Greenhouse Gas Inventories Programme. IGES, Japan.

Klusman, R.W., 2011. Comparison of surface and near-surface geochemical methods for detection of gas microseepage from carbon dioxide sequestration. International Journal of Greenhouse Gas Control 5, 1369–1392.

Klusman, R.W., 2005. Baseline studies of surface gas exchange and soil-gas composition in preparation for CO_2 sequestration research: Teapot Dome, Wyoming. The American Association of Petroleum Geologists. AAPG Bulletin 89, 981–1003.

Klusman, R.W., 2003a. Evaluation of leakage potential from a carbon dioxide EOR/sequestration project. Energy Conversion and Management 44, 1921–1940.

Klusman, R.W., 2003b. Rate measurements and detection of gas microseepage to the atmosphere from an enhanced oil recovery/sequestration project, Rangely, Colorado, USA. Applied Geochemistry 18, 1825–1838.

Klusman, R.W., Moore, J.N., LeRoy, M.P., 2000. Potential for surface gas flux measurements in exploration and surface evaluation of geothermal resources. Geothermics 29, 637–670.

Leuning, R., Etheridge, D., Luhar, A., Dunse, B., 2008. Atmospheric monitoring and verification technologies for CO_2 geosequestration. International Journal of Greenhouse Gas Control 2, 401–414.

Lewicki, J., Bergfeld, D., Cardellini, C., Chiodini, G., Granieri, D., Varley, N., Werner, C., 2005. Comparative soil CO_2 flux measurements and geostatistical estimation. Bulletin of Volcanology 68, 76–90.

Lupion, M., Diego, R., Loubeau, L., Navarrete, B., 2011. CIUDEN CCS project: status of the CO_2 capture technology development plant in power generation. Energy Procedia 4, 5639–5646.

Mazadiego, L.F., Grandía, F., Elío, J., Nissi, B., Vaselli, O., Ortega, M., 2012. Baseline of soil–atmosphere CO_2 flux in the Hontomin site (Burgos, Spain). In: Third EAGE CO2 Geological Storage Workshop, Understanding the Behaviour of CO2 in Geologic Storage Reservoirs, March 26–27, Edinburgh (UK).

Melián, G., Tassi, F., Pérez, N., Hernández, P., Sortino, F., Vaselli, O., Padrón, E., Nolasco, D., Barrancos, J., Padilla, G., Rodríguez, F., Dionis, S., Calvo, D., Notsu, K., Sumino, H., 2012. A magmatic source for fumaroles and diffuse degassing from the summit crater of Teide Volcano (Tenerife, Canary Islands): a geochemical evidence for the 2004–2005 seismic–volcanic crisis. Bulletin of Volcanology 74, 1465–1483.

NETL, 2009. Best practices for: Monitoring, verification, and accounting of CO2 Stored in deep geologic formations. National Energy Technology Laboratory DOE/NETL-311/081508.

Möner, N.-A., Etiope, G., 2002. Carbon degassing from the lithosphere. Global and Planetary Change 33, 185–203.

Nisi, B., Vaselli, O., Tassi, F., Elío, J., Delgado, A., Mazadiego, L.F., Ortega, M.F., 2013. Hydrogeochemistry of running and spring waters in the Hontomín-Huermeces area (Burgos Spain). International Journal of Greenhouse Gas Control 14, 151–168.

Ogaya, X., Ledo, J., Queralt, P., Marcuello, M., Quintà, A., 2013. First geoelectrical image of the subsurface of the Hontomín site (Spain) for CO_2 geological storage: a magnetotelluric 2D characterization. International Journal of Greenhouse Gas Control 13, 168–179.

Pebesma, E.J., 2004. Multivariable geostatistics in S: the gstat package. Computers & Geosciences 30, 683–691.

Permanyer, A., Márquez, G., Gallego, J.R., 2013. Compositional variability in oils and formation waters from the Ayoluengo and Hontomín fields (Burgos, Spain). Implications for assessing biodegradation and reservoir compartmentalization. Organic Geochemistry 54, 125–139.

Pujalte, V., Robles, S., García-Ramos, J.C., Hernández, J.M., 2004. El Malm-Barremiense no marinos de la Cordillera Cantábrica. In: Vera, J.A. (Ed.), Geología de España. SGE-IGME, Madrid, pp. 288–291.

Quesada, S., Robles, S., Rosales, I., 2005. Depositional architecture and transgressive–regressive cycles within Liassic backstepping carbonate ramps in the Basque-Cantabrian basin, northern Spain. Journal of the Geological Society 162, 531–538.

Quesada, S., Dorronsoro, C., Robles, S., 1995. Genetic relationship between the oil of the Ayoluengo field and the Liassic source-rock of the Southwestern Basque-Cantabrian Basin (Northern Spain). In: Grimalt, J.O., Dorronsoro, C. (Eds.), Organic Geochemistry: Developments and Applications to Energy, Climate, Environment and Human History. A.I.G.O.A, Donostia-San Sebastian, pp. 461–463.

Quesada, S., Dorronsoro, C., Robles, S., Chaler, R., Grimalt, J.O., 1997. Geochemical correlation of oil form the Ayoluengo field to Liassic black shale units in the southwestern Basque-Cantabrian Basin (northern Spain). Organic Geochemistry 27, 25–40.

Quesada, S., Robles, S., 1995. Organic geochemistry, distribution and depositional dynamics of the Liassic organic facies of the Basque-Cantabrian Basin (Northern Spain). In: Grimalt, J.O., Dorronsoro, C. (Eds.), Organic Geochemistrw Developments and Applications to Energy, Climate, Environment and Human History. A.1.G.O.A, Donostia-San Sebastian, pp. 464–465.

Quesada, S., Robles, S., Pujalte, V., 1993. E1 Jurásico marino del margen suroccidental de la Cuenca Vasco-Cantábrica y su relación con la explotación de hidrocarburos. Geogaceta 13, 92–96.

Quintà, A., Tavani, S., Roca, E., 2012. Fracture pattern analysis as a tool for constraining the interaction between regional and diapir-related stress fields: Poza de la Sal Diapir (Basque Pyrenees, Spain). Geological Society, London, Special Publications 363, 521–532.

R Core Team, 2012. R: A language and environment for statistical computing. R Foundation for Statistical Computing, Vienna, Austria, ISBN 3-900051-07-0, http://www.R-project.org/

Raich, J.W., Schlesinger, W.H., 1992. The global carbon dioxide flux in soil respiration and its relationship to vegetation and climate. Tellus 44B, 81–99.

Salminen, R., Gregorauskien, V., 2000. Considerations regarding the definition of a geochemical baseline of elements in the surficial materials in areas differing in basic geology. Applied Geochemistry 15, 647–653.

Salminen, R., Tarvainen, T., 1997. The problem of defining geochemical baselines. A case study of selected elements and geological materials in Finland. Journal of Geochemical Exploration 60, 91–98.

Sánchez, M., Ozores, M., López, M., Colle, R., De Torre, B., García, M.A., Pérez, I., 2003. Soil CO_2 fluxes beneath barley on the central Spanish plateau. Agricultural and Forest Meteorology 118, 85–95.

Tarvainen, T., Kallio, E., 2002. Baselines of certain bioavailable and total heavy metal concentrations in Finland. Applied Geochemistry 17, 975–980.

Tavani, S., Quintà, A., Granado, P., 2011. Cenozoic right-lateral wrench tectonics in the Western Pyrenees (Spain): The Ubierna Fault System. Tectonophysics 509, 238–253.

USEPA, 2010. Geologic CO2 Sequestration Technology and Cost Analysis. Office of Water (4606-M). EPA 816-R10-008.